INSTITUTE OF PHYSICS PUBLISHING MEASUREMENT SCIENCE AND TECHNOLOGY
Meas. Sci. Technol. **16** (2005) 191–198 doi:10.1088/0957-0233/16/1/025

Discrete combinatorial investigation of polymer mixture phase boundaries*

João T Cabral and Alamgir Karim

Polymers Division, National Institute of Standards and Technology, Gaithersburg, MD 20899-8542, USA

E-mail: joao.cabral@nist.gov and alamgir.karim@nist.gov

Received 29 April 2004, in final form 29 September 2004
Published 16 December 2004
Online at stacks.iop.org/MST/16/191

Abstract
We report a combinatorial approach for mapping bulk polymer mixture phase behaviour. The technique consists of a parallel cloud point detection scheme using discrete composition libraries, which are scanned across a temperature range and optically imaged. The sample substrates are microwell arrays fabricated by contact photolithography on a glass coverslip. Polymer blend libraries are generated using a custom built, programmable liquid dispenser system. The sample arrays are placed in a uniform, but continuously varying, temperature field, causing the mixture to traverse its phase boundary. Optical turbidity is detected by imaging the entire array and the cloud point curve is determined through automated parallel image analysis. The entire process is simple, flexible, inexpensive and rapid. In this demonstration, we investigate two binary mixtures of low molecular mass poly(styrene) and poly(butadiene), exhibiting upper critical solution temperature (UCST) phase behaviour. The cloud point curves obtained closely approximate the bulk binodal line, and have a high composition resolution of $\delta\phi = 0.01$ (volume fraction), using 10×10 sample arrays. We discuss the potential and limitations of this high throughput methodology for other polymeric mixtures, including multi-component systems.

Keywords: polymer mixtures, combinatorial methods, miscibility, phase separation, turbidity

M This article features online multimedia enhancements

(Some figures in this article are in colour only in the electronic version)

1. Introduction

Pure polymers are rarely used in practical applications. Instead, polymeric materials are generally mixtures of several components: polymers, fillers, compatibilizers, processing aids, etc (Utracki 1989, Paul and Bucknall 1999). The properties of a mixture result from a complex interplay, sometimes synergistic, of the individual component properties. Blending two or more polymers provides an inexpensive, yet powerful, route to materials development and fine-tuning of specific properties. However, polymer miscibility is normally limited, given the small entropy gain involved in mixing long macromolecules.

Polymer mixture thermodynamics and phase behaviour have both practical and fundamental importance. However, no general treatment of polymer miscibility exists and predicting phase behaviour remains a theoretical challenge. A starting point is the classic Flory–Huggins theory (Flory 1955), which captures important trends of miscibility. This mean-field lattice theory assumes a combinatorial entropy of mixing ΔS_m and an enthalpic term ΔH_m which characterizes the interaction *strength* by the χ parameter. The free energy of mixing ΔG_m of polymers A and B is written as

$$\frac{\Delta G_m}{k_B T} = \frac{\phi}{v_A N_A} \ln \phi + \frac{(1-\phi)}{v_B N_B} \ln(1-\phi) + \frac{\phi(1-\phi)}{v} \chi, \quad (1)$$

* Contribution of the National Institute of Standards and Technology, not subject to copyright in the United States.

where $\phi, N_{A,B}$ and $v_{A,B}$ are, respectively, the volume fraction, the degree of polymerization and the monomer molar volumes of polymers A and B (with $\phi_B = 1 - \phi_A$); v is a reference volume and k_B is the Boltzmann constant. In the simplest case, χ is inversely proportional to temperature and independent of $N_{A,B}$ or ϕ. However, chain architecture and connectivity, specific interactions and compressibility generally give rise to additional complexity (Balsara 1996, Dudowicz *et al* 2002, and references therein).

The phase boundaries of mixtures are calculated according to the stability to concentration fluctuations using classical thermodynamics. The binodal line, separating the one- and two-phase regions, is defined by an equilibrium condition between coexisting phases and must be computed numerically. The spinodal delineates the unstable region and is given by

$$\chi_S(T) = \frac{v}{2}\left[\frac{1}{N_A v_A \phi} + \frac{1}{N_B v_B (1-\phi)}\right]. \qquad (2)$$

The volume fractions of the resulting phases are computed from the binodal and from the conservation of the overall mixture composition, at a given temperature. Component polydispersity is common in practical applications and brings additional complexity to phase behaviour (Stockmayer 1949, Koningsveld and Staverman 1968, Šolc 1970, 1975, Roe and Lu 1985). The mechanisms and kinetics of phase separation via spinodal decomposition and nucleation and growth (in the metastable region) have been reviewed by Gunton *et al* (1983) and Hashimoto (1988).

A variety of experimental techniques can be employed to probe bulk phase boundaries and demixing processes (Olabisi *et al* 1979), each with an inherent spatial scale, time resolution and source of contrast. They can be divided into real- and reciprocal-space techniques. The former encompass optical, electron and atomic force microscopy while the latter include scattering techniques using light, neutron and x-ray radiation (for example, Higgins and Benoit 1994, Cabral *et al* 2001, 2002). Spectroscopic or calorimetric techniques can also tackle aspects of polymer miscibility. Here, we are concerned with optical detection (microscopy, turbidity and scattering) for which the source of contrast is a difference in refractive index between the components of the mixture. When annealed inside the two-phase region, thermal composition fluctuations drive a homogeneous mixture to decompose in two coexisting phases. The evolution in time of the amplitude and wavelength of such fluctuations depends on the efficient mechanism of phase separation and structure coarsening. When the size of the composition heterogeneities becomes comparable to the wavelength of light, the mixture appears 'turbid' or 'cloudy' due to scattered light. The onset of turbidity is the 'cloud point' CP. The cloud point temperature, T_{CP}, is determined during a temperature scan of a mixture from the one-phase into the two-phase region, at a given rate. Given the kinetic nature of phase separation, T_{CP} is generally a function of the heating (for lower critical solution temperature mixtures LCST) or cooling (upper critical solution temperature UCST) measurement rate.

The complex dependence of mixture phase boundaries on specific polymer parameters (size distribution, architecture, specific interactions) and the limited predictive ability of available theories demand novel, fast and accurate screening tools for polymer mixture phase behaviour. Meredith *et al* (2000) reported an elegant measurement scheme on thin polymer films with a continuous gradient in composition subjected to an orthogonal temperature gradient. A film (300 nm to 500 nm) was deposited by flow coating a solution of poly(styrene) and poly(vinyl methyl ether) with regularly varying composition. The cloud point curve was obtained by annealing from a single library specimen on a 90 °C $< T <$ 160 °C gradient. In this work, we develop an alternative, complementary, high-throughput phase mapping approach.

We report cloud point measurements on *discrete*, rather than *continuous*, composition libraries, which are annealed on a uniform, but temporally varying, temperature field. The motivations of such a discretization approach are several: (i) an enlargement of the available parameter space, as libraries of more than two components can be produced; (ii) the study of phase separation in the bulk, rather than in thin films which are known to be affected by surface interactions (Sung *et al* 1996, and references therein); (iii) the investigation of low molecular mass mixtures or rubbery polymers at room temperature, whose large mobility would disrupt a composition gradient; (iv) the immobilization of composition libraries which permits multiple, reversible, experimentation; and (v) the elimination of possible complications involving physical processes driven by composition (and thickness) gradients. With these ideas in mind, we fabricate suitable combinatorial sample substrates, a discrete library deposition methodology and a parallel cloud point detection scheme. We demonstrate our technique using a well-known upper critical solution temperature mixture of poly(styrene) and poly(butadiene) of low molecular weight (Roe and Zin 1980, Lin *et al* 1985, Tomlins and Higgins 1989, Sung and Han 1995).

2. Experimental details

2.1. Polymer mixtures

Two mixtures of poly(styrene), PS, and poly(butadiene), PB, molecular mass standards were employed in this combinatorial cloud point curve measurement demonstration. The first mixture, labelled PS2.4K/PB2.8K, consisted of PS with relative molecular mass $M_{r,w} = 2.43$ kg mol^{-1} and polydispersity index $M_{r,w}/M_{r,n} = 1.1$ (Aldrich) and PB $M_{r,w} = 2.8$ kg mol^{-1} (Goodyear). The second mixture, labelled PS2.8K/PB1K was PS with $M_{r,w} = 2.78$ kg mol^{-1} and $M_{r,w}/M_{r,n} = 1.09$ (Polymer Source) and PB $M_{r,w} = 1.0$ kg mol^{-1}, $M_{r,w}/M_{r,n} = 1.2$ (Polysciences). Typical microstructures for anionic polymerizations of PB, although not determined for these specific samples, are 90% 1, 4 (50% trans and 40% cis) with 10% 1, 2 addition. The polymer standards were dissolved in 50/50 mass fraction solutions with toluene (Baker, 99.9%) and stirred for several hours at room temperature. The polymer mixture libraries were generated using a custom built liquid dispenser described below.

2.2. Microwell substrates

Library substrates were fabricated using a contact photolithography methodology described earlier

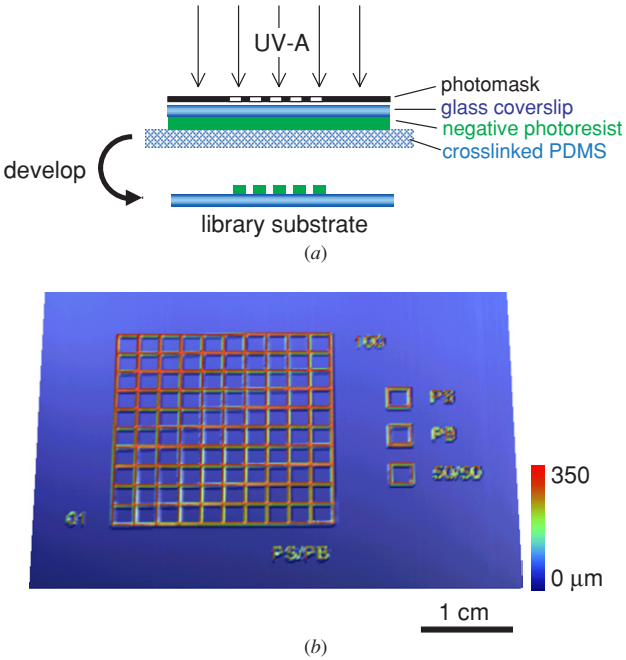

Figure 1. Library substrate. (*a*) Schematic of the microwell array fabrication process by contact lithography of a polymeric photoresist material. The lateral dimensions are fixed by the photomask while the frontal photopolymerization process defines the vertical dimensions. (*b*) Profilometry scan of a typical microarray containing 10 × 10 sample microwells (of 1 μL each), three additional fiduciary wells (for pure components and 50/50 mixture) and patterned reference labels.

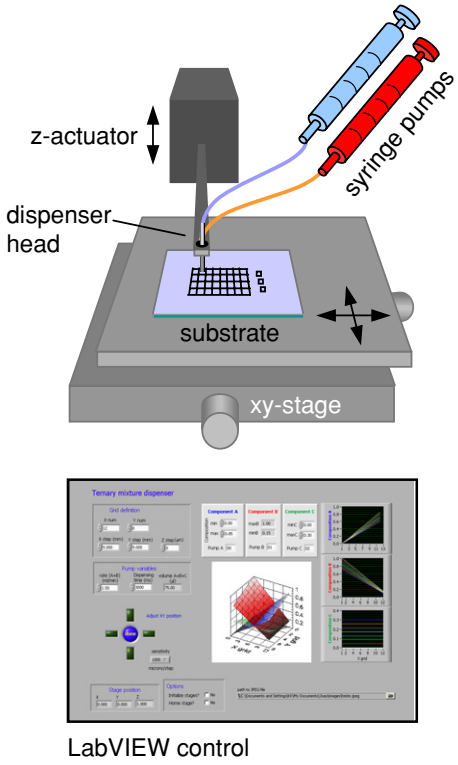

Figure 2. Library fabrication. Schematic of the home-built liquid dispenser, consisting of a series of motorized fluid pumps and stages, computer-controlled using LabVIEW.

(Harrison *et al* 2004, Cabral *et al* 2004). A negative polymer resist is exposed through a photomask resulting in an array of microwells patterned on a glass plate. The set-up is depicted in figure 1(*a*). The light source was a 365 nm ultraviolet (UV-A) Spectroline SB-100P flood lamp (Spectronics, NY). The photomask was designed with a conventional graphics package (e.g., Canvas 7, Deneba) and is printed on a transparency (CG3300, 3M) using a 1200 dpi laser printer (Laserjet 8000N, Hewlett Packard). The glass substrates were 45 cm × 50 cm, 150 μm thick coverslips (Fisher, PA). The photoresist was a multifunctional thiolene based optical adhesive NOA81 (Norland Products). This liquid pre-polymer cures into a hard solid network with considerable resistance to organic solvents, including toluene. The bottom (release) surface consisted of a crosslinked poly(dimethyl siloxane) elastomer Sylgard 184 (Dow Corning, MI) with 10 : 1 mass ratio of base to curing agent and cured for 1 h at 75 °C. The pre-polymer resin was sandwiched between the glass and PDMS surfaces separated by a 500 μm thick spacer (silicon wafer slivers) and UV exposed to approximately 25 mJ cm^{-2} (about 5 min using an intensity of 150 μW cm^{-2}). This exposure dose is chosen to accurately determine the patterned height in this frontal photopolymerization process (Cabral *et al* 2004). Typical height uncertainty is less than 5%. The glass coverslip was slowly separated from the PDMS surface and the uncrosslinked material was washed away using a 50/50 (mass fraction) ethanol/acetone mixture and by blowing compressed nitrogen. The patterned resist on glass was post-cured using an additional UV dose of 1.0 J cm^{-2}. The overall process requires less than 15 min. An optional thermal cure (12 h at 50 °C) extends the durability of the pattern.

The resulting sample substrate was imaged using a stylus profilometer (Dektak 8 equipped with a 12.5 μm tip, Veeco, CA) and is shown in figure 1(*b*). It consists of a 10 × 10 array of microwells, 2 mm × 2 mm wide and 350 μm tall, yielding a 1.4 μL sample volume per well. These dimensions are defined by the photomask and light exposition and can be readily modified to suit other specifications. In addition, three individual sample wells (labelled 'PS', 'PB' and '50/50') serve as fiduciary or reference points. For convenience, the substrate is identified ('PS/PB') and the first and last microwells labelled ('01' and '100') by the lithographic process.

2.3. *Library fabrication*

A home-built programmable liquid dispensing system was employed to prepare discrete polymer mixture libraries. It consists of a series of computer controlled syringe pumps and motorized stages, as depicted in figure 2. The *dispenser head* consists of an aluminium platform to which stainless steel needles (gauge 26, Hamilton) are attached and mounted normal to the sample surface. The microwell substrate is placed on the xy stage under the dispenser head and aligned with the stage's axis. The xy translation stage is made of two linear stages ILS150CC (Newport, CA) stacked orthogonal to each other. The dispenser head is motorized vertically

(along the z-axis) by a linear actuator 850G (Newport, CA). Both stages and actuator are connected to a motor driver UNIDRIV6000 and ESP6000-SYS-6 controller (Newport, CA). Air tight (500 or 1000) μL syringes are loaded with the polymer solutions, secured onto BS8000 fluid pumps (New Era, NY), and connected to the dispenser head by Teflon capillaries (Hamilton). A desktop computer equipped with LabVIEW (National Instruments, TX) controls both the fluid pumps and the motion stages. Additional syringe pumps (up to 99) can be installed in series to produce multi-component libraries.

The library is generated from left-to-right, in successive lines from bottom-to-top (cf figure 1(b)). Deposition proceeds as follows: (i) the stages move to an appropriate xy coordinate, placing the dispensing head above a microwell, (ii) the liquid pumps deliver a calculated amount of both inputs, (iii) the z-actuator brings the needles down, in contact with the substrate, (iv) the liquid mixture is deposited and (v) the actuator returns to its position. The near-contact of the needles with the substrate glass allows the dispensing of small volumes (of the order of 0.1 μL to 1 μL) which are key for this application. Typical vertical travel of the dispensing tip is $\Delta z \approx$ (800 to 1500) μm.

The first and last microwells, labelled '01' and '100', contain the end point compositions in a given range. In this case, these are the pure components. The composition of intermediate samples is a linear combination of both inputs, keeping the dispensed volume constant (1.4 μL, in this case). In a 10 $\times$ 10 library, the nominal composition step is 1% volume fraction. The accuracy of the composition library depends on numerous factors, including the resolution of the syringe pump stepper motors, the diameter of the syringe barrel and dispenser tip contamination. The first two determine the minimum dispensable volume (a 'quantum'). Our choice of parameters brings this value below 1/100 of the well volume. The latter can be minimized by tuning Δz such that the needles are never immersed in the sample but come in sufficient contact with the surface for liquid transfer to occur. Sample positioning (xyz) is accurate to approximately 1 μm and therefore exceeds the requirements of this application. Perhaps the major limitation of the methodology is that the viscosity of the component liquids should be kept relatively low (up to $\approx$1 Pa s) so that dispensing is accurate and subsequent sample homogenization (via diffusion, usually at elevated temperature) is efficient.

The home-built dispenser described here readily fabricates multi-component liquid mixtures within minutes (typical dispensing time per well is 1 s to 5 s, plus a few seconds of stage motion). In this work, we fabricated two libraries of 100 compositions from concentrated PS and PB solutions in toluene. Additional reference samples were prepared and dispensed manually. Sample compositions are given by volume fraction of the components. The mixtures phase-separate upon evaporation of toluene at room temperature. Thorough solvent drying and mixture homogenization were carried out under vacuum (10 Pa, approximately 10^{-1} mbar) at 25 °C above the bulk critical temperature, T_C (139 °C for PS2.4K/PB2.8K and 107 °C for PS2.8K/PB1K), for 2 h. The libraries were then rapidly transferred to the cloud point measurement set-up, kept above T_C.

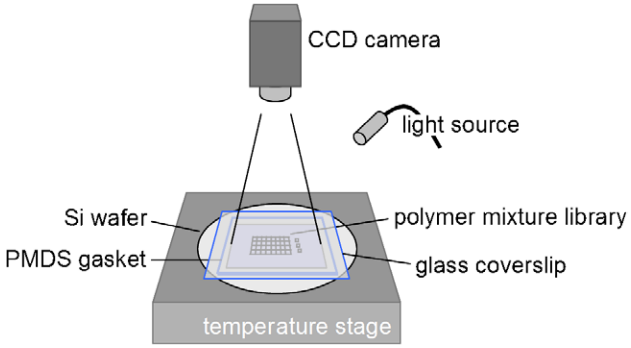

Figure 3. Cloud point detection set-up. Schematic of the parallel turbidity experiments, depicting the microwell array on a temperature controlled hot stage. The sample is supported by a reflective silicon wafer, for improved conductivity and optical contrast, and enclosed within a gasket and transparent window to minimize thermal convection. The entire array is imaged during the CP experiment, at a given frequency, using a CCD camera and fibre-optic illumination.

2.4. Cloud point detection

The phase boundaries were monitored optically while cooling the entire library from above the mixture's critical temperature down to room temperature at a controlled rate. A schematic of the experimental set-up utilized is given in figure 3. The glass coverslip supporting the sample library is placed on a silicon wafer (10 cm diameter, 400 μm thick, Wafer World, FL) and onto a hot stage equipped with a PID controller and type K thermocouples. A thin (1 mm) PDMS gasket was placed around the sample and covered with a glass plate 75 mm $\times$ 50 mm $\times$ 1 mm (Corning Microslides). The entire set-up was covered with aluminium foil (functioning as a thermal screen) with the exception of the observation area. A standard 8 bit, 470 $\times$ 704 pixel black & white progressive CCD camera TM-9700 (Pulnix, CA) was mounted on a lab stand and focused on the library surface. A fibre-optic light source was placed at an angle near the surface normal but without reflecting directly onto the CCD lens. The light intensity was adjusted for maximum optical contrast. Image acquisition was carried out using LabVIEW running on a desktop computer.

The efficiency of this CP detection scheme requires (i) a homogeneous temperature field, experienced by all samples, which can be controlled in time at a known rate and (ii) a high image contrast, with sensitivity to the onset of phase separation. The silicon wafer under the library exhibits large thermal conduction and light reflectance, serving both purposes. The sample environment is thermally isolated by the thick top glass plate and PDMS gasket, minimizing convection in the narrow experimental chamber, and additional aluminium foil shield. The bottom glass substrate in contact with the silicon wafer is, on the other hand, only 150 μm thick allowing for rapid equilibration of the sample temperature. The homogeneity of the temperature was monitored with an infrared thermometer (Oakton, IL) and found to be better than 0.2 °C over the 2.4 cm $\times$ 2.4 cm area occupied by the library.

The experimental procedure was rather simple. The samples were heated above the mixture's critical temperature, until all 100 compositions appeared clear. The equilibration (and homogeneity) of the system was verified by the reversibility of phase separation. The temperature was cycled

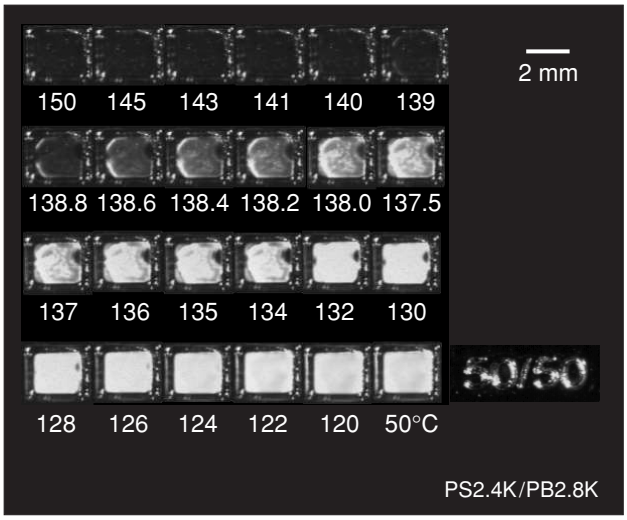

Figure 4. Single microwell turbidity experiment of a 50/50 volume fraction PS2.4K/PB2.8K mixture. The sample was first homogenized above the critical temperature and cooled down, at a rate of 1 °C min^{-1}, while acquiring image at given intervals (ranging from 0.2 °C to 1 °C). Only selected images are shown, in particular near the CP temperature.

M An AVI movie of this figure is available from stacks.iop.org/MST/16/191

several times near the turbidity onset and the location of the phase boundary was consistently verified. The sample library was then cooled from the homogeneous state down to room temperature at a constant rate of 1 °C min^{-1}, while acquiring images every 0.2 °C and then every 1 °C. The image analysis and CP determination are described in the following section.

3. Results and discussion

Combinatorial and high-throughput approaches generate large amounts of data and require efficient data mining. The feasibility of the designed experimental protocol was therefore first validated through inspection of two major issues: single microwell cloud point detection (data acquisition) and automated image analysis (data mining) prior to the actual phase behaviour study on libraries.

The detection scheme is demonstrated on a single microwell sample, which was chosen to be the fiduciary 50/50 composition of one representative system (PS2.4K/PB2.8K). The optical reflection of the sample, detected while cooling down from 150 °C to 50 °C at 1 °C min^{-1}, is shown in figure 4. From direct visual inspection, the CP temperature of this mixture (at this cooling rate) is found to be between 140 °C and 138 °C. In the interest of measurement accuracy and applicability to combinatorial library examination, we sought to establish a precise criterion for CP detection based on image analysis. By integrating the light intensity inside the microwell as a function of temperature, the CP temperature was defined as the onset of intensity rise. We have employed a common graphics and programming package, IGOR Pro 4 (WaveMetrics, OR), for image analysis automation. Our procedure works as follows. The first image is loaded and a region of interest (ROI) (i.e., the area delimited by the microwell), is defined by the user. The remaining steps

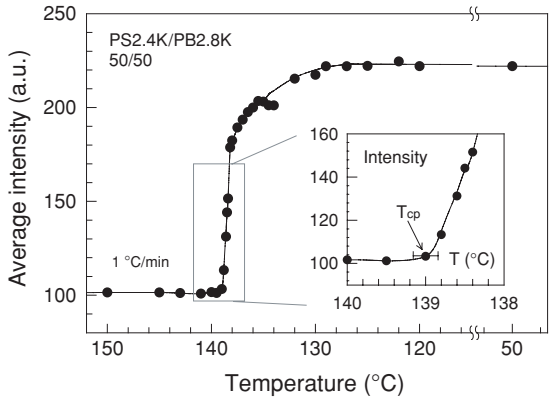

Figure 5. Automated CP image analysis of the data shown in figure 4. The light intensity inside the 50/50 PS/PB fiduciary microwell is computed, averaged across the region of interest and plotted against experimental temperature. The line is a guide to the eye. The CP temperature is defined by the onset of the intensity increase and found to be (139.0 ± 0.2) °C, as shown in the inset.

proceed automatically. The intensity level inside the ROI is averaged (integrated and divided by pixel number) and plotted against the experimental temperature (encoded in the file name). The subsequent images are loaded and the intensity is averaged, keeping the defined ROI. The data pairs— reflected average intensity $\langle I \rangle$ and temperature T— are collected and plotted together. The output of the data analysis of the 50/50 mixture (images in figure 4) is shown in figure 5. The intensity data are obtained in relative units and scaled with $2^8 = 256$ grey levels, since the images were acquired in 8 bit format. At high temperatures, the mixture is transparent (appears black in reflection) and therefore the intensity is low. The average intensity reading (of approximately 100) corresponds to the background and does not change with temperature in the one-phase region. Upon cooling, phase separation initiates, resulting in optical turbidity (the image appears white) and consequent rise of intensity. The value saturates at $\langle I \rangle \approx 225$, corresponding to maximum optical contrast between phases, and then decreases slightly as coarsening proceeds. The 'cloud point' temperature is defined as the first intensity departure from the baseline, beyond experimental uncertainty. We find T_{CP} (50/50) = (139.0 ± 0.2) °C for this mixture, depicted in the inset of figure 5.

The success of this automated image analysis is predicated upon having (i) constant illumination throughout the experiment and (ii) stable sample positioning with respect to the CCD camera. The former permits direct comparison of light intensities (in *relative* units) reflected from the microwells during the course of the experiment. The latter allows the utilization of a single ROI for integration of all images for each microwell.

Having demonstrated CP experiments and automated analysis on single microwells, we now consider larger combinatorial libraries of mixtures. The turbidity of a 100 microwell library of PS2.8K/PB1K while cooling into the two-phase region is shown in figure 6 for selected temperatures (movie in supporting information). As mentioned earlier, the library is organized starting from the bottom left microwell, containing pure PB, to the top right corner, which contains pure PS. The PS/PB ratio increases from left to right (along lines)

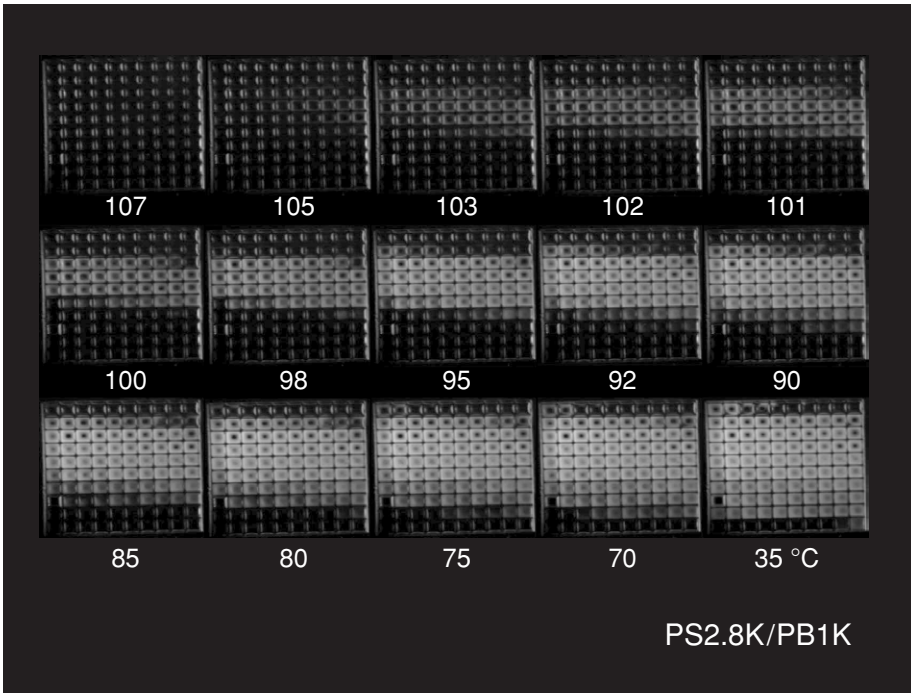

Figure 6. Multiwell CP experiment of 10 × 10 compositions of the PS2.8K/PB1K system. The bottom left and top right corners correspond to pure PB and PS, respectively. The array was equilibrated in that phase region and imaged during a controlled cooling down to room temperature. Selected images are shown.

M An AVI movie of this figure is available from stacks.iop.org/MST/16/191

and from bottom to top. Other library designs can be used, as long as the sample compositions are adequately referenced. The efficiency of this approach is evident from the selective onset of turbidity: first near the centre of the array and finally near the pure component edges. Some asymmetry is visible and is expected from the molecular mass difference between the components.

Automated data mining is more challenging when imaging large areas. In this experiment, each microwell corresponds only to 30 × 30 pixels of the whole image. As a result, statistical averaging of the reflected intensity is noisier and sample position stability is critical. We demonstrate here that both conditions can be satisfied with our simple experimental set-up (figure 3). The data analysis of the whole library is a trivial extension of the single microwell case. As before, upon loading the first image, the user defines a ROI for a *single* microwell. The remaining 99 ROIs are computed from the geometric parameters of the sample array. For convenience of this procedure, the microwell array should be aligned parallel to the image frame, at the beginning of the experiment. The subsequent steps—(i) intensity averaging, (ii) plotting of $\langle I \rangle$ versus T and (iii) CP computation—proceed in parallel for all library samples.

Close inspection of figure 6 suggests possible concerns about the accuracy of our image analysis-based cloud point determination. Firstly, the turbidity contrast inside the microwells appears to be non-uniform and a transparent 'hole' forms near the centre of the cells. However, the variation in contrast is only due to sample thickness: as the scattering volume decreases, films appear less opaque and eventually transparent below a certain detection threshold. As the mixtures preferentially wet the edges of the array, the film thickness profile becomes a concave meniscus, thinner and therefore more 'transparent' near the centre. This artefact does not affect our analysis scheme other than by reducing the optical contrast between homogeneous (clear) and phase-separated (turbid) samples. Several attempts have been made to minimize this effect, including tuning of microwell vertical dimensions and dispensing volumes, and modification of the surface energy of the substrate (glass and/or grid matrix). Care should be taken in choosing an optimal sample thickness for CP detection. We have found that (100 to 200) μm thick films were suitable for our measurements. In the interest of simplicity and in order to demonstrate the robustness of our approach, we have used unmodified substrates in the data shown in figure 6.

The optical contrast of phase-separating mixtures depends on several factors, in addition to the scattering volume of the sample and inherent refractive index difference between components, discussed above. In particular, it is a function of the composition difference and relative volume fraction of the two resulting phases. A near-critical composition quenched near the phase boundaries yields two mixed phases of nearly identical composition and hence, with minimal refractive index contrast. On the other hand, off-critical mixtures quenched near the phase boundaries yield two phases with a large disparity in volume fraction and, hence, weakly scattering. These limitations are inherent to demixing processes. In the particular case of this mixture, in which the glass transition temperature T_g of one component (PS) lies close to the phase boundaries, the reduction in mobility may interfere with the CP detection of mixture compositions approaching the pure component PS.

A recurrent concern when employing combinatorial and high-throughput techniques, whether using continuous or

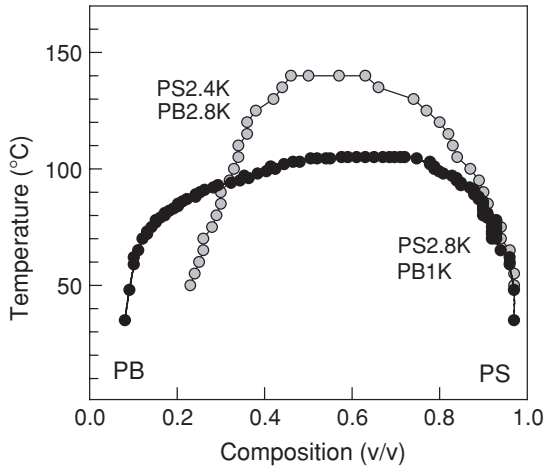

Figure 7. Cloud point curves obtained for mixtures (○) PS2.4K/PB2.8K and (●) PS2.8K/PB1K using the combinatorial microwell CP approach. Automated parallel image analysis of the entire sample array was carried out as a function of measurement temperature. Each datum results from a scan of average intensity $\langle I \rangle$ versus temperature T, as shown in figure 5. The composition resolution is $\delta\phi = 0.01$ volume fraction and the temperature accuracy is given by a combination of cooling and image acquisition rates and optical contrast.

discrete libraries, is the accuracy and calibration of samples arrays and the possibility of errors in the library generation. We have addressed the former by adjusting the dispensing resolution to be above the target composition step and by validating the final library by FT-IR spectroscopy. As a consequence, we are able to utilize the nominal mixture composition without calibrating each specimen individually. Accidental errors, on the other hand, may be more difficult to eliminate, but have little influence on the overall result. As an example, composition PS/PB 0.20/0.80 (microwell reference 21, bottom left) in the array shown in figure 6 was not dispensed adequately. However, this missing datum represents only a 0.01 PS/PB volume fraction jump in the phase boundary and therefore does not affect the accuracy of the measurement significantly.

Figure 7 summarizes the CP experimental results from the two poly(styrene)/poly(butadiene) mixtures investigated: PS2.4K/PB2.8K and PS2.8K/PB1K. The measurements agree well with the available literature (Roe and Zin 1980, Lin *et al* 1985, Tomlins and Higgins 1989, Sung and Han 1995). Each point corresponds to a microwell sample scanned in temperature and analysed according to the procedure described above. The resolution in temperature (vertical axis) is determined by the cooling rate and image acquisition frequency. Standard T_{CP} uncertainty is less than 1 °C. The resolution in composition (horizontal axis) is defined by the sample number and concentration range explored. At each temperature, 100 compositions (for these particular sample arrays) were probed for miscibility. We are not aware of any cloud point measurements in the literature with better composition resolution.

The phase boundaries of a polymer mixture are fully defined by the thermodynamically significant spinodal and binodal lines. The 'cloud point curve' is strictly the onset of turbidity at a certain heating/cooling rate (for LCST/UCST mixtures). Due to the kinetic nature of phase separation, the process is initiated at the phase boundary but only detected inside the metastable or even unstable regions, in particular for viscous solutions. Measurements of CP curves at various rates allow for an extrapolation of the zero-rate cloud point and therefore an estimation of the binodal line. In the particular case of the low $M_{r,w}$ polymer mixture studied, the rate employed is slow enough for quasi-static measurements given the high mobility of the components. Decreasing the cooling rate did not have an effect on the CP curve beyond our measurement accuracy, indicative of a close approximation of the binodal line. However, a determination of the spinodal line requires temperature-jump experiments inside the unstable region while monitoring the structure factor (via scattering) or microstructure (via microscopy) of the mixture as it evolves from homogeneous to heterogeneous. Such experiments are in progress.

Finally, we discuss the range of application of the high-throughput CP detection scheme reported here. Our library fabrication procedure relies on precision dispensing of pure components (assisted by a common solvent) followed by sample homogenization via diffusion in the one-phase region. Therefore, the procedure is best suited for UCST mixtures, which can be homogenized at high temperatures and then cooled down for CP determination. However, the method is applicable to either LCST or UCST mixtures with an accessible one-phase region in which both polymers have sufficient mobility to inter-diffuse and form a homogeneous blend in thermodynamic equilibrium.

4. Conclusion

We report a novel combinatorial measurement scheme for polymer mixture phase behaviour. This approach encompasses substrate design and fabrication, library generation, automated cloud point detection and data processing. Each step of the process is rather simple, flexible and inexpensive. Their combination is shown to provide a powerful measurement tool for polymer mixture phase boundaries.

The sample substrates are fabricated using a rapid prototyping technique based on contact photolithography of multifunctional polymer resists. Regular arrays of microwells with controlled lateral and vertical dimensions are readily produced. The polymer mixture libraries are generated using a home-built liquid dispensing system, consisting of a series of motorized and computer-controlled syringe pumps and motion stages. We have employed approximately 50 μL (or 50 mg) of polymer per array. The cloud point temperatures of the entire sample array were measured simultaneously while scanning temperature across the phase boundaries. Only a standard CCD camera, hot stage and a graphics computer package are required. The final cloud point curve is obtained by parallel image analysis and data processing. We have employed mixtures of model poly(styrene) and poly(butadiene) in this demonstration, obtaining unprecedented resolution in sample composition using arrays of 10×10 microwells.

The microwell array dimension and discretization are tailored for specific applications. Typically, a compromise between sample volume reduction and detection sensitivity is necessary. In the cloud point experiments reported here,

an upper limit for array size is dictated by the requirement of temperature uniformity across the sample area. A lower limit stems from the optical contrast dependence on scattering volume. In addition, the study of 'bulk' phase separation requires a significantly large sample size with respect to the range of surface interactions (e.g., preferential wetting of surfaces by mixture components). Indeed, the process exhibits a qualitatively different nature upon confinement, i.e., for thicknesses below $\approx$0.1 μm (Sung *et al* 1996, and references therein). Sample discretization is carried out based on the dependence of the measurement property on the experimental variables, keeping a balance between accuracy and reasonable data mining. In our case, T_{CP} varies slowly with mixture composition ϕ but the overall binodal line shape is a complex function of the polymer molecular mass distributions, therefore requiring multiple data points.

The methodology demonstrated here with *binary* mixtures can be easily extended to *multi-component* systems, which exhibit additional phase behaviour complexity. Combinatorial and high-throughput measurements will become critical, not only for fast screening and exploratory phase boundary determination but also in measurement refinement and elucidation of sharp transitions, such as around a critical micelle concentration of a copolymer solution.

Acknowledgments

The authors thank Jack F Douglas (NIST) for numerous discussions, Kapeeleshwar Krishana (Rhodia, NJ) for assistance in developing the liquid dispenser and Adel Halasa (Goodyear, OH) for a kind donation of one poly(butadiene) specimen. JTC thanks NIST for a Foreign Guest Researcher fellowship.

Disclaimer

Certain commercial equipment, instruments, or materials are identified in this paper in order to specify the experimental procedure adequately. Such identification is not intended to imply recommendation or endorsement by the National Institute of Standards and Technology, nor is it intended to imply that the materials or equipment identified are necessarily the best available for the purpose.

References

Balsara N P 1996 Thermodynamics of polymer blends *Physical Properties of Polymer Handbook* ed J E Mark (Woodbury, NY: AIP) chapter 19 pp 257–68

Cabral J T, Higgins J S, McLeish T C B, Strausser S and Magonov S N 2001 Bulk spinodal decomposition studied by atomic force microscopy and light scattering *Macromolecules* **34** 3748–56

Cabral J T, Higgins J S, Yerina N A and Magonov S N 2002 Topography of phase separated critical and off-critical polymer mixtures *Macromolecules* **35** 1941–50

Cabral J T, Hudson S D, Harrison C and Douglas J F 2004 Frontal photopolymerization for microfluidic applications *Langmuir* **20** 10020–9

Dudowicz J, Freed K F and Douglas J F 2002 Beyond Flory–Huggins theory: new classes of blend miscibility associated with monomer structural asymmetry *Phys. Rev. Lett.* **88** 095503

Flory P J 1955 *Principles of Polymer Chemistry* (Ithaca, NY: Cornell University Press)

Gunton J D, San-Miguel M and Sahni P S 1983 The dynamics of first-order phase transitions *Phase Transitions and Critical Phenomena* vol 8 ed C Domb and J L Lebowitz (New York: Academic) pp 267–482

Harrison C, Cabral J T, Stafford C, Karim A and Amis E J 2004 A rapid prototyping technique for the fabrication of solvent resistant structures *J. Micromech. Microeng.* **14** 153–8

Hashimoto T 1988 Dynamics in spinodal decomposition of polymer mixtures *Phase Transit.* **12** 47–119

Higgins J S and Benoit H C 1994 *Polymers and Neutron Scattering* (Oxford: Clarendon)

Koningsveld R and Staverman A J 1968 Liquid–liquid phase separation in multicomponent polymer solutions: III. Cloud-point curves *J. Polym. Sci.* A-2 **6** 349–66

Lin J-L, Rigby D and Roe R-J 1985 Deuterium isotope effect on the compatibility between polystyrene and polybutadiene *Macromolecules* **18** 1609–11

Meredith J C, Karim A and Amis E J 2000 High-throughput measurement of polymer blend phase behavior *Macromolecules* **33** 5760–2

Olabisi O, Robertson L M and Shaw M T 1979 *Polymer–Polymer Miscibility* (New York: Academic)

Paul D R and Bucknall C B (ed) 1999 *Polymer Blends* (New York: Wiley)

Roe R-J and Lu L 1985 Effect of polydispersity on the cloud-point curves of polymer mixtures *J. Polym. Sci.: Polym. Phys.* **23** 917–24

Roe R-J and Zin W-C 1980 Determination of the polymer–polymer interaction parameter for the polystyrene–polybutadiene pair *Macromolecules* **13** 1221–8

Šolc K 1970 Cloud-point curves of polymer solutions *Macromolecules* **3** 665–73

Šolc K 1975 Cloud-point curves of polymers with logarithmic-normal distribution of molecular weight *Macromolecules* **8** 819–27

Stockmayer W H 1949 Solubility of heterogeneous polymers *J. Chem. Phys.* **17** 588

Sung L and Han C C 1995 Light-scattering studies on phase separation in a binary blend with addition of block copolymers *J. Polym. Sci.: B Polym. Phys.* **33** 2405–12

Sung L, Karim A, Douglas J F and Han C C 1996 Dimensional crossover in the phase separation of thin polymer blend films *Phys. Rev. Lett.* **76** 4368–71

Tomlins P E and Higgins J S 1989 Late stage spinodal decomposition in an oligomeric blend of polystyrene/polybutadiene: a test of the scaling law for the structure function *J. Chem. Phys.* **90** 6691–700

Utracki L A 1989 *Polymer Alloys and Blends: Thermodynamics and Rheology* (Munich: Hanser)